Expedited Simulation-Driven Design Optimization of UWB Antennas By Means of Response Features

Slawomir Koziel and Adrian Bekasiewicz

Engineering Optimization & Modeling Center, School of Science and Engineering, Reykjavík University, Menntavegur 1, 101 Reykjavík, Iceland
(koziel@ru.is, bekasiewicz@ru.is)

Keywords: Antenna design, UWB antennas, design optimization, simulation-driven design, response features, feature-based optimization, surrogate modeling.

Abstract

In this work, a method for fast design optimization of broadband antennas is considered. The approach is based on a feature-based optimization (FBO) concept where reflection characteristics of the structure at hand are formulated in terms of suitably defined feature points. Redefinition of the design problem allows for reducing the design optimization cost, because the dependence of feature point coordinates on antenna dimensions is less nonlinear than for the original frequency characteristics (here, *S*-parameters). This results in faster convergence of the optimization algorithm. The cost of the design process is further reduced using variable-fidelity electromagnetic (EM) simulation models. In case of UWB antennas, the feature points are defined, among others, as the levels of the reflection characteristic at its local in-band maxima, as well as location of the frequency point which corresponds to acceptable reflection around the lower corner frequency within the UWB band. Also, the number of characteristic points depends on antenna topology and its dimensions. Performance of FBO-based design optimization is demonstrated using two examples of planar UWB antennas. Moreover, the computational cost of the approach is compared to conventional optimization driven by a pattern search algorithm. Experimental validation of the numerical results is also provided.

1. Introduction

Full-wave electromagnetic (EM) simulations have become one of the most important tools in the design of modern antennas. Clearly, one of the reasons is fast development and availability of hardware and specialized software. Another and perhaps even more important reason is practical necessity. Contemporary structures including compact antennas [1], [2] dielectric resonator antennas [3], and others can be accurately evaluated only using versatile, yet expensive EM analysis. The reason is that simpler (hence, computationally cheaper) models either, such as equivalent circuits, do not exist or cannot provide acceptable accuracy. Moreover, performance of the antenna accompanied with its closest environment (e.g., housing [4], connectors [1]) can only be evaluated through EM simulations. In many situations it is mandatory: for example, the SMA connector may affect the performance of compact UWB antenna in a very significant way [1], [5] so that it needs to be included into the computational model to ensure reliable design.

One of the key problems related to EM-driven antenna design is high cost of accurate simulations [6], [7]. Another problem is a large number of geometry parameters that need to be simultaneously adjusted [7]. Altogether, these factors create considerable challenges especially for numerical optimization where a large number of EM model evaluations of are normally necessary. Conventional gradient-based [8] or derivative free [9] algorithms may require hundreds of simulations to converge, whereas global methods such as population-based metaheuristics [10]-[13] involve thousands of model evaluations. Consequently, their utilization for optimization of antenna structure is infeasible cost-wise. At the same time, interactive design procedures (still dominant in both academia and industry) based on parameter sweeps driven by engineering experience can handle only one or two parameters at a time [14], [15]. As a result, they cannot lead to truly optimum designs.

Research efforts towards reducing the numerical cost of simulation-driven design optimization processes are mostly focused on surrogate-based optimization (SBO) methods [16]-[19] which are probably the most promising approaches developed so far. The SBO methods that utilize physics-based surrogates seem to be advantageous. The combination of

knowledge embedded in the low-fidelity antenna model and its speed allows for considerable reduction of the number of simulations required by the optimization method to converge. The most promising SBO methods that exploit physical models include, among others, space mapping [19], shape-preserving response prediction (SPRP) [20], adaptive response correction [21], manifold mapping [22], and adaptively adjusted design specifications [23]. Another popular approach for reducing the computational cost of gradient-based optimization is utilization of adjoint sensitivities [24]-[26]. Combinations of physics-based SBO with adjoint sensitivities have also been reported (e.g., adjoint-based space mapping [27], or adjoint-enhanced SPRP [28]). However, availability of adjoint sensitivity in commercial EM solvers is not yet widespread.

Feature-based optimization—originally developed for microwave filters [29] and integrated photonic components [30]—belongs to the most recent methods that permit efficient EM-driven design. The key idea behind FBO is reformulation of the design problem at hand in a so-called feature space. The functional landscape of the latter is less nonlinear than that in the original formulation. Preliminary work on application of the response features for optimization of broadband antennas has been presented in [31]. For wideband structures, the definition and extraction of the feature coordinates is more challenging than for narrow-band ones. This is because the lower edge of the antenna bandwidth has to be maintained at acceptable level and the reflection has to be controlled in the entire UWB band. Furthermore, the number of feature points (specifically, the number of local maxima) may change depending on the particular antenna geometry and its dimensions. This potential variability has been handled through appropriately developed algorithm. In this work, the method of [31] is utilized for the design of two numerically challenging EM models of UWB monopole antennas. In each case, the FBO-driven design has been performed at a cost corresponding to only a few dozen of EM simulations of the respectively antenna. The FBO approach has been also compared to conventional pattern search-based optimization in terms of numerical cost. The simulation results are supported by measurement data.

2. UWB Antenna Design Using Response Features

In this section, we recall the formulation of the feature-based optimization algorithm.

Moreover, we briefly outline the approach utilized to define and identify feature points of the UWB antenna responses. The section is concluded with a description of the practical issues related to implementation of the feature-based approach for optimization of UWB structures.

2.1. Response Features for UWB Antennas

Frequency responses of an exemplary UWB antenna (here, the uniplanar structure considered as one of the examples) are shown in Fig. 1. Normally, the antenna design specifications can be fulfilled or not based on the following properties of the response: (i) reflection levels for the in-band maxima and at the upper corner frequency, and (ii) allocation of the frequency point at which $|S_{11}| \leq -10$ dB right before the first resonance of the response. It should be noted, however, that the reference level for (ii) can be set to a lower value in order to ensure a safety margin. Also, as shown in Fig. 1(a), such a point may not exist. Moreover, the number of reflection maxima may change with the antenna geometry (cf. Fig. 1.(c)). These situations are handled by the algorithm of Section 2.2.

2.2. UWB Antenna Design Problem in the Feature Space

Although extraction of the response features may be challenging, reformulation of the problem in terms of the frequency f_k and level l_k of the suitably defined feature points (k = 1, …, K) is advantageous. The reason is that the feature points change less nonlinearly with the antenna dimensions than the frequency response [29], [30]. As a result, faster convergence of the optimization algorithm can be expected.

Conventional formulation of the design problem is given by

$$\boldsymbol{x}^* = \arg\min_{\boldsymbol{x}} U(\boldsymbol{R}_f(\boldsymbol{x})) \tag{1}$$

where U is the objective function defined as $U(\boldsymbol{R}_f(\boldsymbol{x})) = \max\{|S_{11}|(\boldsymbol{x})_{3.1\text{ GHz to }10.6\text{ GHz}}\}$ and $\boldsymbol{R}_f$ is the response of an accurate high-fidelity EM antenna model. The aim of FBO is to reformulate (1) in terms of the feature points. The vectors of frequency and level coordinates are denoted by $\boldsymbol{F}(\boldsymbol{x}) = [f_1(\boldsymbol{x})\ \ f_2(\boldsymbol{x})\ \ \ldots\ f_K(\boldsymbol{x})]^T$, and $\boldsymbol{L}(\boldsymbol{x}) = [l_1(\boldsymbol{x})\ \ l_2(\boldsymbol{x})\ \ \ldots\ l_K(\boldsymbol{x})]^T$, respectively. The reformulated design problem is as follows

$$\boldsymbol{x}^* = \arg\min_{\boldsymbol{x}} U_F(\boldsymbol{F}(\boldsymbol{x}), \boldsymbol{L}(\boldsymbol{x})) \tag{2}$$

where U_F is the objective function defined for the extracted features of the response.

As mentioned before, the first feature point for UWB structures $[f_1,l_1]$ corresponds to the lowest frequency f_1 at which it attains the reference level l_1 (here, –15 dB; cf. Section 2.1). If the reflection level at the first resonance is above l_1, the first feature point is defined as the reflection level and frequency at the first resonance.

The remaining are defined as described in Section 2.1. The in-band reflection level and allocation of the f_1 point are controlled using the following objective function

$$U_F(\boldsymbol{x}) = \max\{l_2(\boldsymbol{x}),...,l_K(\boldsymbol{x})\} + \beta\left[(\max\{f_1 - f_{1.\text{target}}, 0\}) / f_{1.\text{target}}\right]^2 \tag{3}$$

where $f_{1.\text{target}}$ = 3.1 GHz stands for the lower edge of the UWB band and β is a penalty coefficient (here, we use β = 1000).

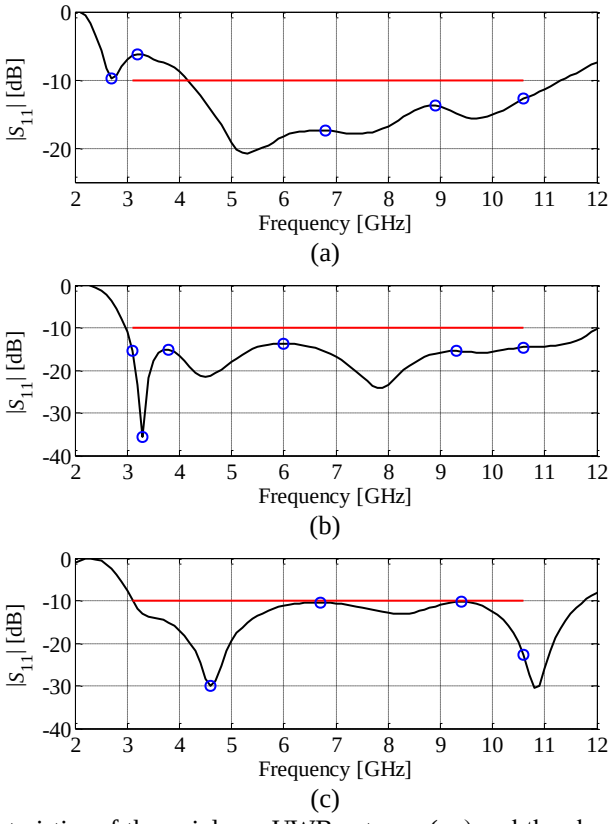

Fig. 1. Reflection characteristics of the uniplanar UWB antenna (—) and the characteristic points (○) utilized by feature-based optimization algorithm: (a) poor design which lacks the –15 dB characteristic point, (b) good design with existing –15 dB point which can be exploited to control the lower corner frequency of the antenna frequency band, (c) design with two local maxima in the frequency band of interest. Note that the thick horizontal line defines design specifications, i.e., $|S_{11}| \leq$ –10 dB within 3.1 GHz to 10.6 GHz band.

In case of violating the desired reflection level for the first resonance, the objective function (3) is automatically switched to the following one

$$U_F(\boldsymbol{x}) = \max\{l_1(\boldsymbol{x}) + 5, l_2(\boldsymbol{x}), ..., l_K(\boldsymbol{x})\} \tag{4}$$

The term $l_1(\boldsymbol{x})$ + 5 in (4) is used to enforce the –15 dB level of the first resonance as opposed to –10 dB required for remaining feature coordinates. For more detailed description of the method see [31].

2.3. Optimization Algorithm

The design problem (2) is solved iteratively as

$$\boldsymbol{x}^{(i+1)} = \arg\min_{\|\boldsymbol{x}-\boldsymbol{x}^{(i)}\| \le r^{(i)}} U_F(\boldsymbol{F}_S^{(i)}(\boldsymbol{x}), \boldsymbol{L}_S^{(i)}(\boldsymbol{x})) \tag{5}$$

with $\boldsymbol{x}^{(i)}$, i = 0, 1, …, being approximations to the final design $\boldsymbol{x}^*$. The vectors $\boldsymbol{F}$ and $\boldsymbol{L}$ in (2) are substituted by their linear approximation models $\boldsymbol{F}_S^{(i)}$ and $\boldsymbol{L}_S^{(i)}$ obtained using finite differentiation (n perturbations around design $\boldsymbol{x}^{(i)}$). The features $\boldsymbol{F}(\boldsymbol{x}^{(i)} + \boldsymbol{h}_k)$, $\boldsymbol{L}(\boldsymbol{x}^{(i)} + \boldsymbol{h}_k)$ ($\boldsymbol{h}_k = [0 \ \ldots \ 0 \ d_k \ 0 \ \ldots \ 0]^T$, k = 1, …, n, $d_k > 0$.) are extracted from the respective frequency responses. The model for frequency features is

$$\boldsymbol{L}_S^{(i)}(\boldsymbol{x}) = \boldsymbol{L}(\boldsymbol{x}^{(i)}) + \begin{bmatrix} [\boldsymbol{L}(\boldsymbol{x}^{(i)} + \boldsymbol{h}_1) - \boldsymbol{L}(\boldsymbol{x}^{(i)})]^T / d_1 \\ \ldots \\ [\boldsymbol{L}(\boldsymbol{x}^{(i)} + \boldsymbol{h}_n) - \boldsymbol{L}(\boldsymbol{x}^{(i)})]^T / d_n \end{bmatrix}^T \cdot (\boldsymbol{x} - \boldsymbol{x}^{(i)}) \tag{6}$$

A similar formula holds for $\boldsymbol{F}_S^{(i)}$. Low cost of the process is ensured by performing finite differentiation at the low-fidelity model level $\boldsymbol{R}_c$ of the antenna at hand. Note that (5) is embedded in a trust-region framework to improve convergence. More detailed discussion on FBO can be found in, e.g., [29], [31], [32], [33].

2.4. Practical Issues

There are two practical issues concerning implementation of the FBO algorithm described in this section. The first one is extraction of the feature points from the $|S_{11}|$ response of the antenna of interest. This can be done easily by scanning the response from the lowest towards the highest frequency and detecting the location of the first resonance, as well as all subsequent local maxima. In our implementation, an appropriate routine is written in Matlab [34].

The second issue is the fact that the number of relevant feature points may change in the course of optimization run. In practice, it is not a problem though because the linear approximation models $\boldsymbol{F}_S^{(i)}$ and $\boldsymbol{L}_S^{(i)}$ are determined at a current point $\boldsymbol{x}^{(i)}$ using small perturbations with respect to $\boldsymbol{x}^{(i)}$. This virtually guarantees feature point consistency for the purpose of approximation model construction. In case the number of feature points changes at the new design $\boldsymbol{x}^{(i+1)}$, the subsequent approximation models are determined using the "new" feature set.

3. Case Studies

In this section, the proposed feature-based design optimization is illustrated using two design examples: an 11-parameter uniplanar UWB antenna fed through a coplanar waveguide (CPW) [35] and a 7-variable rectangular-shaped UWB monopole [36]. The feature-based algorithm is compared with conventional optimization approach in terms of the computational cost. Moreover, the last two antenna structures are validated through measurements of their optimized designs.

3.1. Case I: Uniplanar UWB Antenna with CPW feed

Consider the uniplanar UWB antenna shown in Fig. 2 [35]. The structure consists of a fork-shaped driven element and a ground plane with open slot. It is fed through the CPW line. As previously, the antenna is designed on a 0.762 mm thick Taconic RF-35. The adjustable parameters are $\boldsymbol{x} = [l_0\ l_1\ l_{2r}\ l_{3r}\ l_4\ l_5\ w_1\ w_2\ w_3\ w_4\ g]^T$. Dimensions $w_f = 3.5$ and $s = 0.16$ are constant to ensure 50 ohm input impedance of the feed line. Relative variables are $l_2 = (0.5w_f + s + w_1)\cdot\max\{l_{2r}, l_{3r}\}$ and $l_3 = (0.5w_f + s + w_1)\cdot l_{3r}$. All dimensions except l_{2r} and l_{3r} are in mm. The ranges of design variables are $\boldsymbol{l}$ = [5 15 0.2 0.2 4 8 7 0.5 0.2 0.2 0.2]^T and $\boldsymbol{u}$ = [15 25 1 0.8 11 16 15 3.5 2.5 2 2]^T.

Two models of the structure have been implemented in the CST Microwave Studio and simulated using its transient solver [37]. The high-fidelity model $\boldsymbol{R}_f$ includes 6,800,000 mesh cells (simulation time: 36 minutes), whereas its low-fidelity counterpart contains ~1,200,000 cells (CPU-time: 198 seconds). For the sake of reliable comparison of the simulation and measurement results, the antenna model is supplemented with the SMA connector.

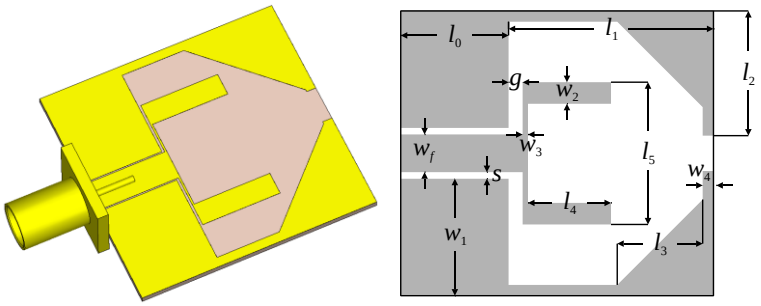

(a) (b)

Fig. 2. Uniplanar UWB antenna: (a) 3D view; (b) geometrical details.

The considered antenna structure has been optimized with respect to two objectives: (i) minimization of reflection (see Section 2.2), and, (ii) size reduction while ensuring acceptable electrical performance (i.e., $|S_{11}| \leq -10$ dB in 3.1 GHz to 10.6 GHz band). The latter is controlled using the following objective function:

$$U_F(\boldsymbol{x}) = A(\boldsymbol{x}) + \beta_1\left[(\max\{l_2(\boldsymbol{x}),...,l_K(\boldsymbol{x})\}+10)/10\right]^2 + \\ + \beta_2\left[(\max\{f_1 - f_{1.\text{target}},0\})/\ f_{1.\text{target}}\right]^2 \tag{7}$$

where $A(\boldsymbol{x})$ is the antenna size, whereas the penalty factors are enforcing the antenna reflection response to stay below –10 dB level within the UWB band (see Section 2.2 for explanation of symbols pertaining to response features).

The initial design for FBO is $\boldsymbol{x}^0$ = [10 19 0.8 0.6 7.7 12 11.3 2 0.5 1 0.8]^T. The final design optimized with respect to reflection is $\boldsymbol{x}^*$ = [9.29 18.36 0.76 0.75 8.93 16 11.41 2.64 0.22 1.09 0.26]^T. It has been obtained after 12 iterations of (5). The dimensions of the optimized structure are 26.6 mm × 27.7 mm and its footprint is 737 mm^2. For the area-wise optimization, the initial design is set to $\boldsymbol{x}^0 = \boldsymbol{x}^*$. The final design $\boldsymbol{x}^{**}$ = [4.86 14.86 0.92 0.59 8.57 14.72 6.68 2.8 0.57 0.2 0.31]^T has been obtained after 15 iterations of the algorithm. The size of the structure at $\boldsymbol{x}^{**}$ is 17.2 mm × 19.7 mm = 339 mm^2 and it is 54% smaller compared to $\boldsymbol{x}^*$. The reflection responses of the antenna structure at the initial and optimized designs are shown in Fig. 3.

The reflection-wise antenna optimization cost corresponds to 25.3 simulations of the high-fidelity model $\boldsymbol{R}_f$, whereas—for the footprint-oriented optimization—the design cost is about 31.3 $\boldsymbol{R}_f$ simulations. Both optimizations have been also performed using the pattern search method [38]. The numerical cost for the $|S_{11}|$- and area-wise FBO design is 321 and 478 simulations of the high-fidelity model. A detailed cost breakdown is provided in Table 1.

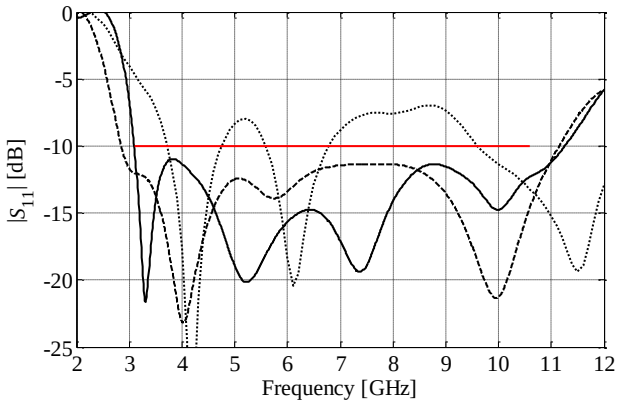

Fig. 3. Uniplanar UWB antenna characteristics at: the initial design (····), reflection-wise optimized design (- - -), and the design optimized with respect to size (—).

Table 1: Uniplanar UWB Antenna: Optimization Cost Breakdown

Optimization Method	Design Objective	Number of Model Evaluations		Total Cost	
		Low-fidelity	High-fidelity	Absolute [hours]	Relative to $\boldsymbol{R}_f$
FBO (this work)	$\|S_{11}\|$	$134 \times \boldsymbol{R}_c$	$13 \times \boldsymbol{R}_f$	15.2	25.3
	Size	$167 \times \boldsymbol{R}_c$	$16 \times \boldsymbol{R}_f$	18.8	31.3
Pattern Search [38]	$\|S_{11}\|$	-	$321 \times \boldsymbol{R}_f$	192.6	321
	Size	-	$478 \times \boldsymbol{R}_f$	286.8	478

The optimized antenna designs have been experimentally validated. The photographs of the fabricated structures are shown in Fig. 4, whereas their simulated and measured performance characteristics are compared in Fig. 5. For the response of Fig. 5(a), the simulated and measured peak in-band reflection is –11.4 dB and –10.7 dB, respectively. Additionally, the measured antenna response is characterized by slightly narrower –10 dB bandwidth (7.8 GHz) with respect to results obtained in the course of simulation (8.3 GHz). For the antenna response shown in Fig. 5(b), the peak reflection is –10.2 for simulation and –10 for measurement. The measured bandwidth is 100 MHz broader than the simulated one. The discrepancies between the characteristics are mostly due to fabrication tolerances as well as the influence of electrically large measurement setup and lack of cable current suppressor [39]. Overall, the agreement between the simulated and the measured antenna responses is acceptable.

A comparison of the E-field radiation patterns (E-plane) for the reflection- and size-oriented design is shown in Fig. 6. As expected, the small antenna exhibits more

omnidirectional properties for lower frequencies. This is a consequence of the radiation pattern being a Fourier transform of the field in the antenna aperture [40]. Thus, the antenna field response becomes narrower with the increasing size.

3.2. Case II: UWB Antenna with Rectangular Radiator

Our second example is the UWB monopole with a rectangular-shaped radiator fed through the microstrip line (see Fig. 7) [36]. Similarly as the antenna of Section 3.1, the structure contains the modified ground plane with L-shaped stub aimed at enhancement of the current path. The design parameters are $\boldsymbol{x} = [l_0\ g\ a\ l_1\ l_2\ w_1\ o]^T$. We also have $w_0 = 2o + a$, whereas the feed line width $w_f = 1.7$ ensures 50 ohm input impedance (all are in mm). The search space of the structure is defined by $\boldsymbol{l} = [4\ {-2}\ 4\ 5\ 1\ 0.5\ 0.5]^T$ and $\boldsymbol{u} = [15\ 2\ 15\ 20\ 10\ 3.5\ 5.5]^T$.

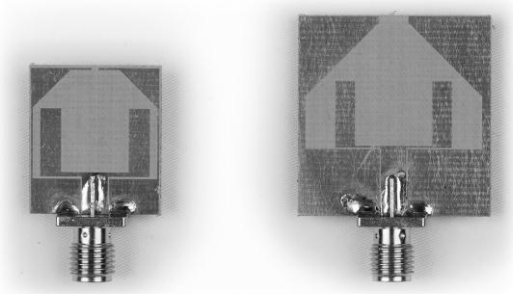

(a) (b)

Fig. 4. Uniplanar UWB antenna: photographs of designs optimized w.r.t: (a) size; and (b) in-band reflection.

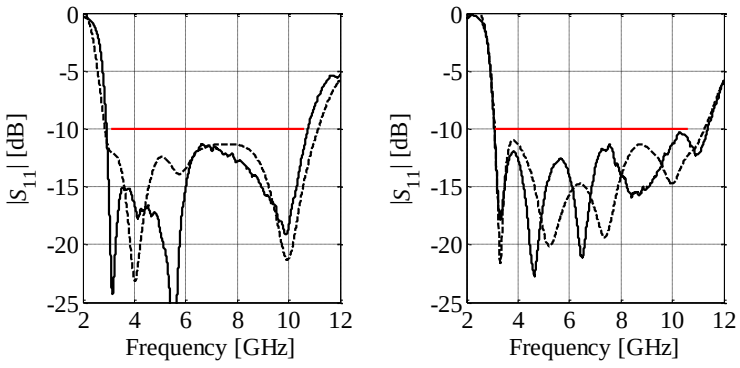

Fig. 5. Comparison of simulated (- - -) and measured (—) reflection characteristics of the uniplanar antenna at the designs optimized w.r.t.: (a) in-band reflection, and (b) size.

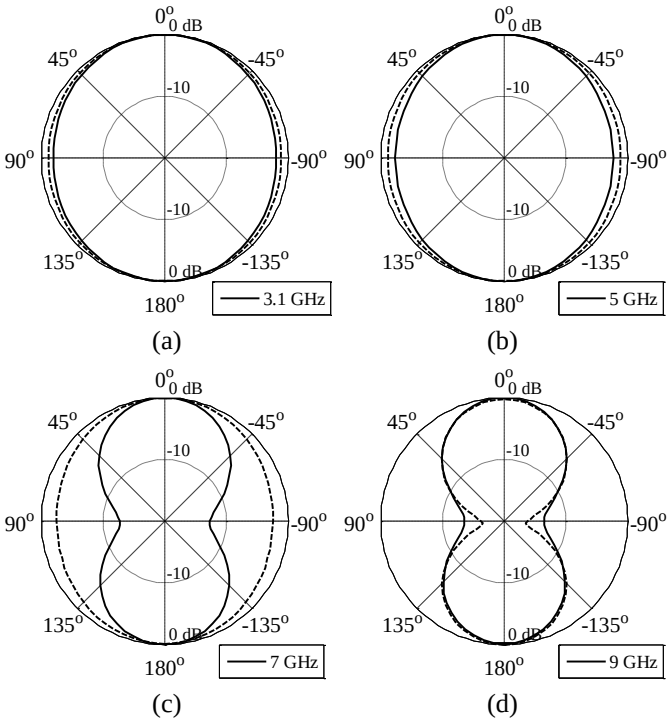

Fig. 6. E-field radiation patterns of the uniplanar UWB antenna obtained for the reflection- (—) and size-wise (– –) optimized designs.

The high- and low-fidelity EM antenna models are both implemented in CST Microwave Studio ($\boldsymbol{R}_f$: ~4,600,000 mesh cells, simulation time 40 minutes, and $\boldsymbol{R}_c$: ~850,000 cells, 2 minutes) [37]. As in Section 3.2, the models are supplemented with SMA connectors to ensure reliable simulation results.

The antenna has been optimized with respect to reflection and size. The design objectives for both cases are defined in Sections 2.2 and 3.2, respectively. For the reflection-wise optimization, the initial design is $\boldsymbol{x}^0 = [7\ 1\ 10\ 11\ 3\ 1\ 1]^T$. The optimal parameter set $\boldsymbol{x}^* = [4.73\ 1.15\ 9.74\ 13.76\ 4.88\ 2.96\ 3.38]^T$ has been obtained after 10 iterations of the FBO algorithm. The antenna dimensions are 16.5 mm × 21.4 mm = 354 mm^2. For the size-oriented design, the initial geometry is set to $\boldsymbol{x}^0 = \boldsymbol{x}^*$. The optimal parameter set $\boldsymbol{x}^{**} = [4.57\ 1.29\ 9\ 13.18\ 6.32\ 1.35\ 1.96]^T$ with corresponding antenna size of 12.9 mm × 19 mm = 247 mm^2 (over 30% smaller compared to $\boldsymbol{x}^*$). The design $\boldsymbol{x}^{**}$ has been obtained in 13 FBO iterations. Figure 8 provides reflection characteristics at the initial and the optimized designs.

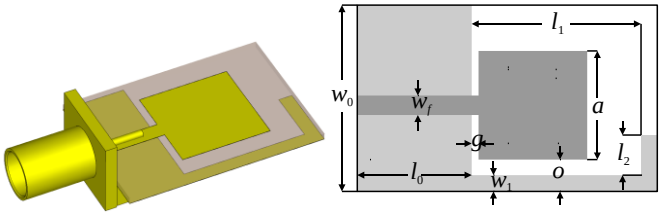

(a) (b)

Fig. 7. UWB monopole with rectangular radiator: (a) 3D view; (b) geometrical details.

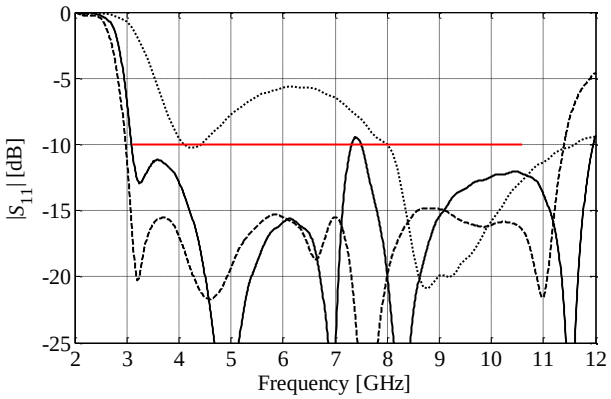

Fig. 8. Rectangular UWB monopole characteristics at: the initial design (····), reflection-wise optimized design (- - -), and the design optimized with respect to size (—).

The numerical cost of the monopole design corresponds to 14.6 and 18.6 evaluations of the high-fidelity model for the reflection- and size-oriented optimization, respectively. At the same time, the cost of pattern-search-based design is 231 and 324 $\boldsymbol{R}_f$ simulations. A detailed cost breakdown is gathered in Table 2.

The obtained antenna designs have been fabricated and measured. The photographs of the manufactured structures are shown in Fig. 9. Figure 10 provides comparisons of simulated and measured reflection characteristics of both designs. For the first case (see Fig. 10(a)), the peak in-band reflection is –14.8 dB and –14.1 dB for simulation and measurement, respectively. Simulated and measured responses of the second design (cf. Fig. 10(b)) are –9.2 dB and –9.4 dB. Overall, the results are acceptable.

Figure 11 shows radiation patterns of the antenna. Similarly as in Section 3.2, the antenna design optimized for size reduction features slightly more omnidirectional characteristics. However, at 7 GHz frequency this effect is reduced due to increased shielding of the ground plane stub. For the 9 GHz frequency, the characteristics are similar.

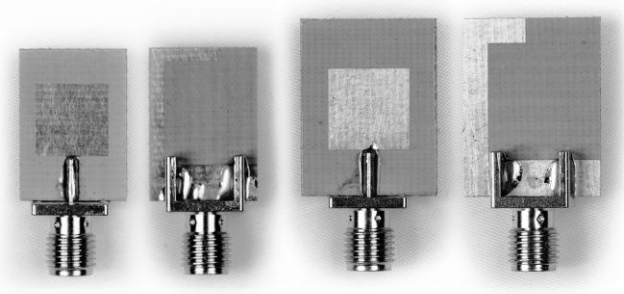

(a) (b)

Fig. 9. Photographs of rectangular monopole designs optimized w.r.t: (a) size; and (b) in-band reflection.

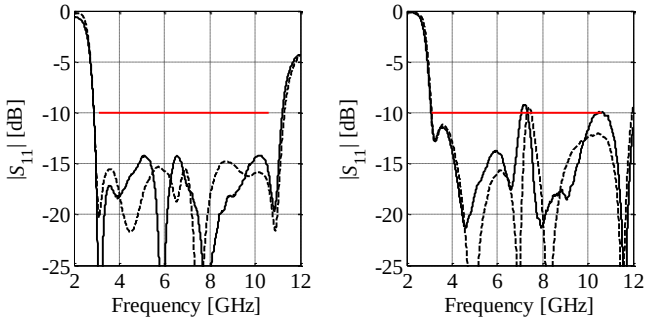

(a) (b)

Fig. 10. Comparison of simulated (- - -) and measured (—) reflection characteristics of the rectangular UWB monopole at the designs optimized w.r.t.: (a) in-band reflection, and (b) size.

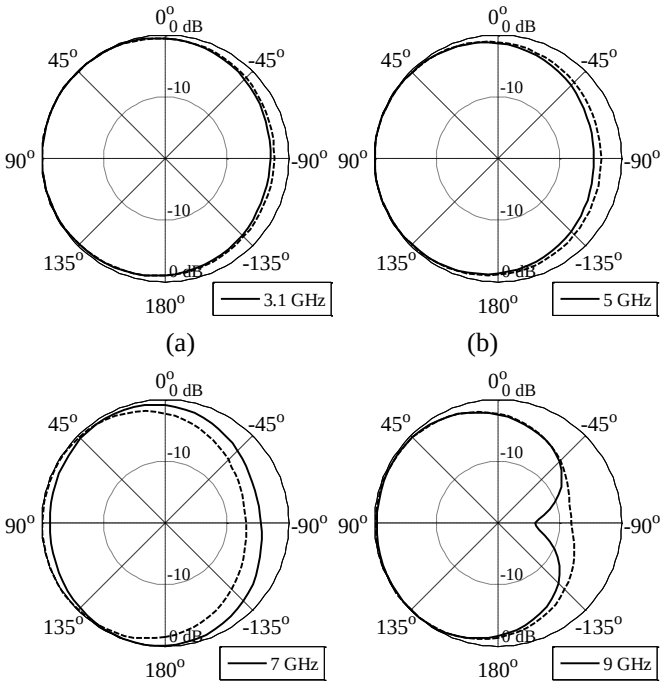

(a) (b)

(c) (d)

Fig. 11. E-plane radiation patterns of the rectangular UWB monopole obtained for the reflection- (—) and size-wise (– –) optimized designs.

Table 2: UWB Monopole with Rectangular Radiator: Optimization Cost Breakdown

Optimization Method	Design Objective	Number of Model Evaluations		Total Cost	
		Low-fidelity	High-fidelity	Absolute [hours]	Relative to $\boldsymbol{R}_f$
FBO (this work)	$\|S_{11}\|$	$72 \times \boldsymbol{R}_c$	$11 \times \boldsymbol{R}_f$	9.7	14.6
	Size	$93 \times \boldsymbol{R}_c$	$14 \times \boldsymbol{R}_f$	12.4	18.6
Pattern Search [38]	$\|S_{11}\|$	-	$231 \times \boldsymbol{R}_f$	154	231
	Size	-	$324 \times \boldsymbol{R}_f$	216	324

5. Conclusion

Rapid design optimization of UWB antennas by means of response features has been considered. Appropriate definition of the objective function allows for simultaneous control of the lower frequency of the antenna response as well as the maximum reflection level within the entire UWB band. As demonstrated through the design of a uniplanar UWB structure, and a rectangular-shaped UWB monopole utilization of response features as well as variable-fidelity EM simulations ensures low cost of the optimization process. Numerical results indicated superiority of the FBO algorithm over conventional techniques, here, pattern search. The considered two antenna examples—four design cases—have been positively verified by means of reflection measurements.

References

[1] A. Bekasiewicz, and S. Koziel, "Structure and computationally-efficient simulation-driven design of compact UWB monopole antenna," *IEEE Ant. Wireless Prop. Lett.*, vol. 14, pp. 1282-1285, 2015.

[2] S. Koziel, S. Ogurtsow, W. Zieniutycz, and A. Bekasiewicz, "Design of a planar UWB dipole antenna with an integrated balun using surrogate-based optimization," *IEEE Ant. Wireless Prop. Lett.*, vol. 14, pp. 366-369, 2015.

[3] A. A. Kishk and Y. M. M. Antar, "Dielectric resonator antennas," in *Antenna Engineering Handbook*, J. L. Volakis, Editor, 4th ed., McGraw-Hill, 2007.

[4] C.C. Lin, S.W. Kuo, and H.R. Chuang, "A 2.4-GHz printed meander-line antenna for USB WLAN with notebook-PC housing," *IEEE Microwave Wireless Comp. Lett.*, vol. 15, no. 9, pp. 546-548, 2005.

[5] D. Pinchera and M.D. Migliore, "A Simple and Effective Procedure for Connector Deembedding in Antenna Arrays," *IEEE Ant. Wireless Prop. Lett.*, vol. 8, pp. 534-537, 2009.

[6] S. Chamaani, M.S. Abrishamian, S.A. Mirtaheri, "Time-domain design of UWB Vivaldi antenna array using multiobjective particle swarm optimization," *IEEE Ant. Wireless Prop. Lett.*, vol. 9, pp. 666-669, 2010.

[7] A. Bekasiewicz and S. Koziel, "Structure and design optimisation of compact UWB slot antenna," *Electronics Lett.*, vol. 52, no. 9, pp. 681-682, 2016.

[8] J. Nocedal and S. Wright, *Numerical Optimization*, 2nd edition, Springer, New York, 2006.

[9] A. Conn, K. Scheinberg, and L.N. Vincente, *Introduction to Derivative-Free Optimization*, MPS-SIAM Series on Optimization, Philadelphia, 2009.

[10] R. L. Haupt, "Antenna design with a mixed integer genetic algorithm," *IEEE Trans. Antennas Propag.*, vol. 55, no. 3, pp. 577–582, Mar. 2007.

[11] M. F. Pantoja, P. Meincke, and A. R. Bretones, "A hybrid genetic algorithm space-mapping tool for the optimization of antennas," *IEEE Trans. Antennas Propag.*, vol. 55, no. 3, pp. 777–781, Mar. 2007.

[12] N. Jin and Y. Rahmat-Samii, "Parallel particle swarm optimization and finite- difference time-domain (PSO/FDTD) algorithm for multiband and wide-band patch antenna designs," *IEEE Trans. Antennas Propag.*, vol. 53, no. 11, pp. 3459–3468, Nov. 2005.

[13] A. Halehdar, D.V. Thiel, A. Lewis, and M. Randall, "Multiobjective optimization of small meander wire dipole antennas in a fixed area using ant colony system," *Int. J. RF and Microwave CAE,* vol. 19, No. 5, pp. 592-597, 2009.

[14] O.M.H. Ahmed, A.R. Sebak, T.A. Denidni, "Compact UWB printed monopole loaded with dielectric resonator antenna," *Electronics Lett.*, vol. 47, no. 1, pp. 7-8, 2011.

[15] C.-Y. Huang, J.-Y. Su, "A printed band-notched UWB antenna using quasi-self-complementary structure," *IEEE Ant. Wireless Prop. Lett.*, vol. 10, pp. 1151-1153, 2011

[16] S. Koziel and S. Ogurtsov, "Antenna design by simulation-driven optimization. Surrogate-based approach," Springer, 2014.

[17] S. Koziel, X.S. Yang, and Q.J. Zhang (Eds.), "Simulation-driven design optimization and modeling for microwave engineering", Imperial College Press, 2013.

[18] N.V. Queipo, R.T. Haftka, W. Shyy, T. Goel, R. Vaidynathan, and P.K. Tucker, "Surrogate-based analysis and optimization," *Progress in Aerospace Sciences*, vol. 41, no. 1, pp. 1-28, Jan. 2005.

[19] J.W. Bandler, Q.S. Cheng, S.A. Dakroury, A.S. Mohamed, M.H. Bakr, K. Madsen, and J. Søndergaard, "Space mapping: the state of the art," *IEEE Trans. Microwave Theory Tech.*, vol. 52, no. 1, pp. 337-361, Jan. 2004.

[20] S. Koziel, S. Ogurtsov, and S. Szczepanski, "Rapid antenna design optimization using shape-preserving response prediction," *Bulletin of the Polish Academy of Sciences. Tech. Sci.*, vol. 60, pp. 143-149, 2012.

[21] S. Koziel, J.W. Bandler, and K. Madsen, "Space mapping with adaptive response correction for microwave design optimization," *IEEE Trans. Microwave Theory Tech.*, vol. 57, no. 2, pp. 478-486, 2009.

[22] S. Koziel, L. Leifsson, and S. Ogurtsov, "Reliable EM-driven microwave design optimization using manifold mapping and adjoint sensitivity," *Microwave Opt. Tech. Lett.*, vol. 55, pp. 809-813, 2013.

[23] S. Koziel and S. Ogurtsov, "Rapid optimization of omnidirectional antennas using adaptively adjusted design specifications and kriging surrogates," *IET Microwaves, Ant. Prop.*, vol. 7, no. 15, pp. 1194-1200, 2013.

[24] M.A. El Sabbagh, M.H. Bakr, and J.W. Bandler, "Adjoint higher order sensitivities for fast full-wave optimization of microwave filters," *IEEE Trans. Microw Theory Tech.*, vol. 54, pp. 3339-3351, 2006.

[25] S. Koziel, and A. Bekasiewicz, "Fast EM-driven size reduction of antenna structures by means of adjoint sensitivities and trust regions," *IEEE Ant. Wireless Prop. Lett.*, vol. 14, pp. 1681-1684, 2015.

[26] M. Ghassemi, M. Bakr and N. Sangary, "Antenna design exploiting adjoint sensitivity-based geometry evolution," *IET Microwaves Ant. Prop.*, vol. 7, no. 4, pp. 268-276, 2013.

[27] A. Khalatpour, R.K. Amineh, Q.S. Cheng, M.H. Bakr, N.K. Nikolova, and J.W. Bandler, "Accelerating space mapping optimization with adjoint sensitivities," *IEEE Microwave Wireless Comp. Lett.*, vol. 21, no. 6, pp. 280-282, 2011.

[28] S. Koziel, S. Ogurtsov, Q.S. Cheng, and J.W. Bandler, "Rapid electromagnetic-based microwave design optimisation exploiting shape-preserving response prediction and adjoint sensitivities," IET Microwaves, Ant. Prop., vol. 8, no. 10, pp. 775-781, 2014.

[29] S. Koziel, and J.W. Bandler, "Rapid Yield Estimation and Optimization of Microwave Structures Exploiting Feature-Based Statistical Analysis," *IEEE Trans. Microwave Theory Tech.*, vol. 63, no. 1, pp. 107-114, 2015.

[30] S. Koziel, S. Ogurtsov, "Fast surrogate-assisted simulation-driven optimisation of add-drop resonators for integrated photonic circuits," *IET Microwaves, Ant. Prop.*, vol. 9, no. 7, pp. 672-675, 2015.

[31] S. Koziel and A. Bekasiewicz, "Fast design optimization of UWB antennas using response features," *Int. Conf. Microwave Radar Wireless Comm.*, pp. 1-4, Krakow, 2016.

[32] O. Glubokov, and S. Koziel, "EM-driven tuning of substrate integrated waveguide filters exploiting feature-space surrogates," *Int. Microwave Symp.*, Tampa Bay, FL, USA, pp. 1-3, 2014.

[33] A.R. Conn, N.I.M. Gould, and P.L. Toint, *Trust Region Methods*, 2000 MPS-SIAM Series on Optimization, 2000.

[34] MathWorks MATLAB, v. 2012a, MathWorks, Inc., 3 Apple Hill Drive, Natick, MA 01760.

[35] X. Qing, Z.N. Chen, "Compact coplanar waveguide-fed ultra-wideband monopole-like slot antenna," *IET Microwaves Ant. Prop.*, vol. 3, no. 5, pp. 889-898, 2009.

[36] S. Koziel, and A. Bekasiewicz, "Low-cost multi-objective optimization of antennas using Pareto front exploration and response features," to appear, *IEEE Int. Symp. Ant. Prop.*, Fajardo, 2016.

[37] CST Microwave Studio, ver. 2013, CST AG, Bad Nauheimer Str. 19, D-64289 Darmstadt, Germany, 2013.

[38] T.G. Kolda, R.M. Lewis, V. Torczon, "Optimization by direct search: new perspectives on some classical and modern methods," *SIAM Review*, vol. 45, no. 3, pp. 385–482, 2003.

[39] T.W. Hertel, "Cable-current effects of miniature UWB antennas," *IEEE Ant. Prop. Society Int. Symp.*, vol. 3A, pp. 524-527, 2005.

[40] C.A. Balanis, *Modern antenna handbook*, John Wiley & Sons, 2008.